Three-dimensional Particle-In-Cell Simulation of a Pulsed Plasma Thruster: Modeling and Challenges

IEPC-2011-116

J. Neudorfer[*]

Institut für Aerodynamik und Gasdynamik, Universität Stuttgart, 70550 Stuttgart, Germany

German Research School for Simulation Sciences GmbH, 52062 Aachen, Germany

T. Stindl[†]

Institut für Raumfahrtsysteme, Universität Stuttgart, 70550 Stuttgart, Germany

R. Schneider[‡]

Karlsruher Institut für Technologie,
Institut für Hochleistungsimpuls- und Mikrowellentechnik, 76021 Karlsruhe, Germany

S. Roller[§]

German Research School for Simulation Sciences GmbH, 52062 Aachen, Germany
Applied Supercomputing in Engineering, RWTH Aachen University, 52062 Aachen, Germany

C.-D. Munz[¶]

Institut für Aerodynamik und Gasdynamik, Universität Stuttgart, 70550 Stuttgart, Germany

and

M. Auweter-Kurtz[‖]

German Aerospace Academy ASA, 71304 Böblingen, Germany

In order to simulate the rarefied plasma flow within pulsed plasma thrusters (PPTs), a fully kinetic approach for the Boltzmann-Maxwell equations is under development by IAG (Institute of Aerodynamics and Gas Dynamics, Universität Stuttgart), IRS (Institute of Space Systems, Universität Stuttgart), ASE (Applied Supercomputing in Engineering, German Research School for Simulation Sciences) and IHM (Institute for Pulsed Power and Microwave Technology, Karlsruher Institut für Technologie). An attractive numerical method to solve the Boltzmann-Maxwell problem without collisions is the Particle-In-Cell method. To additionally take the change of the distribution function due to binary reactions and charged particle Coulomb interactions, i.e. the Boltzmann collision integral, into account, the Direct Simulation Monte Carlo method and a stochastic approach is applied, respectively. However, to simulate a PPT, various additional effects have to be

[*]Scientist, Numerical Methods of Fluid Dynamics, neudorfer@iag.uni-stuttgart.de
[†]Scientist, Space Transportation Technology, stindl@irs.uni-stuttgart.de
[‡]Senior Fellow, Computational Plasma Physics, rudolf.schneider@kit.edu
[§]Professor, Head of Applied Supercomputing in Engineering, s.roller@grs-sim.de
[¶]Professor, Head of Numerical Methods of Fluid Dynamics, munz@iag.uni-stuttgart.de
[‖]Professor, Head of German Aerospace Academy, m.auweter-kurtz@german-asa.de

incorporated. Among these are the current through the electrodes, the electric circuitry including the capacitor, the ablation of the propellant, the emission of electrons at the cathode and more. The approaches and models used are presented and preliminary results and findings are discussed.

Nomenclature

$\vec{B}$	magnetic induction
C	capacitance
d	extent of emission box in x- and z-direction
$\vec{E}$	electric field
$\vec{F}$	Lorentz force
f	distribution function
I	current
$\vec{j}$	current density
m	mass
Q	charge
q	particle charge
t	time
U	voltage
v	velocity
X	charge increment required per unit potential difference

Subscripts

0	initial value
av	averaged
$Coll$	collision
e	electron
i	time interval
k	species index
n	dimension [1,2,3]
pr	prescribed

Greek Symbols

ϵ_0	electric permittivity
ρ	charge density

Abbreviations

ASE	**A**pplied **S**upercomputing in **E**ngineering
DSMC	**D**irect **S**imulation **M**onte **C**arlo
IAG	**I**nstitut für **A**erodynamik und **G**asdynamik (Institute of Aerodynamics and Gasdynamics
IHM	**I**nstitut für **H**ochleistungsimpuls und **M**ikrowellentechnik (Institute of High Power Impulse and Microwave Technology)
IRS	**I**nstitut für **R**aumfahrtsysteme (Institute of Space Systems)
MPF	**M**acro**P**article **F**actor
PIC	**P**article **i**n **C**ell

I.   Introduction

Pulsed Plasma Thrusters (PPTs) of various geometries have been under development at the Institut für Raumfahrtsysteme (IRS, Institute of Space Systems) since 2002.[1] They can generally be used for attitude control, drag compensation and formation flight as well as potential main thruster for long term missions like the planned lunar Mission BW1.[2] In order to supplement experimental PPT development and optimization, a numerical code has been under development. Due to the short duration of a PPT pulse, the high current and the low mass, the plasma flow within the PPT is highly unsteady and rarefied, both of which makes the use of a continuum-based solver unfeasible. Instead, a particle method developed jointly by IAG

(Institute of Aerodynamics and Gas Dynamics, Universität Stuttgart), IRS, ASE (Applied Supercomputing in Engineering, German Research School for Simulation Sciences) and IHM (Institute for Pulsed Power and Microwave Technology, Karlsruher Institut für Technologie) is being used.[3,4] In addition to the plasma flow itself, several boundary conditions and external effects specific to a PPT have to be simulated, namely the current through the electrodes, the discharge circuitry including the capacitor, the voltage applied to the electrodes and others. This paper presents the modeling approaches used and discusses the results. In Section II, the modeling of the various parts is presented, specifically of the plasma itself (II.A), the electric circuitry (II.B), the initial conditions (II.C), the electrode voltage (II.D), the electrode current (II.E) and the electron emissions (II.F). Section III discusses the results of the modeling approaches and Section IV provides conclusions and an outlook to future work.

II.   Modeling

A.   Plasma Modeling

The Boltzmann equation

$$\frac{\partial f_k}{\partial t} + \vec{v}_k \cdot \nabla_x f_k + \frac{\vec{F}_k}{m_k} \cdot \nabla_v f_k = \left(\frac{\delta f_k}{\delta t}\right)_{Coll} \tag{1}$$

describes the change of the distribution function f_k for species k in time and phase space as a result of external and self forces $\vec{F}_k$ and particle collisions, indicated by the Boltzmann collisional integral on the right-hand-side. Since the Boltzmann equation cannot be solved directly, its different parts are decoupled and treated separately. Neglecting collisions, the equation only describes the interaction of charged particles and electromagnetic fields and reduces to the Maxwell-Vlasov equations, which are solved by using a Particle-in-Cell (PIC) method.[5] The PIC scheme implemented uses a discontinuous Galerkin method on a three-dimensional unstructured grid[6] to compute the electromagnetic fields based on the propagation of the fields as defined by Maxwell's equations. Instead of the classical Maxwell equations consisting of two hyperbolic and two elliptic equations, the purely hyperbolic Maxwell model with divergence cleaning[7]

$$\frac{\partial \vec{U}}{\partial t} + \sum_{n=1}^{3} \frac{\partial}{\partial x_n} \left[\mathcal{K}_n \vec{U}\right] = \vec{g}, \tag{2}$$

is implemented, where $\vec{U}$ contains the variables of state $\vec{U}(\vec{x}, t) = (E_x, E_y, E_z, B_x, B_y, B_z, \Psi, \Phi)^T$ with the two additional degrees of freedom Ψ and Φ. $\mathcal{K}_n$ are block-structured matrices with constant entries.[7] The right-hand side of Eq. (2) is essentially given by the particles which act as source terms through the charge and current density ρ and $\vec{j}$ according to

$$\vec{g} = -\frac{1}{\epsilon_0}(j_x, j_y, j_z, 0, 0, 0, -\chi\rho, 0)^T , \tag{3}$$

where χ is an arbitrary constant greater than or equal to one which governs the speed of the divergence cleaning. The computed fields are interpolated to the particle positions using interpolation techniques of different order.[4] The particles are then moved according to the Lorentz force and the resulting charge and current density distributions are deposited as sources into the Maxwell solver again, closing the self-consistent interplay. The collisions are taken into account by coupling the PIC scheme with a Direct Simulation Monte Carlo (DSMC) solver and a stochastic Fokker-Planck solver as schematically depicted in Figure 1. The different solvers have been described in detail in several previous publications.[4,8–11] In the scope of this paper, the collisions are neglected, i.e. the DSMC and Fokker-Planck algorithms are not used in the present context.
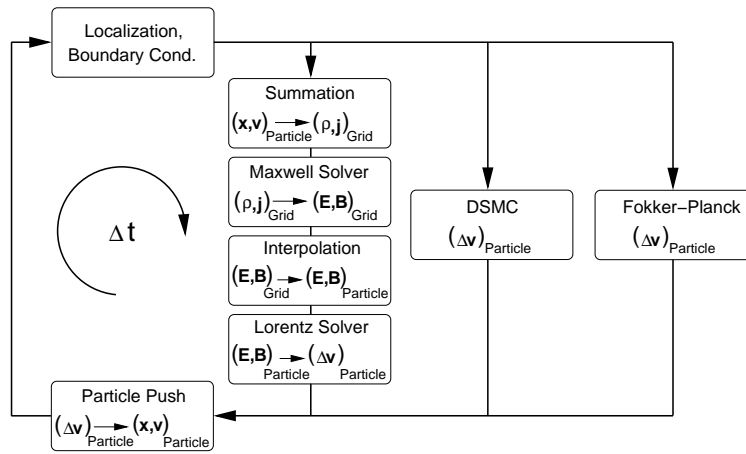
Figure 1. Depiction of the coupling scheme (timestep)

B. Electric Circuitry

The energy for the PPT developed at IRS is usually provided by a capacitor, which is connected to the electrodes and to a power supply. The capacitor is charged with an initial voltage U_0. A spark plug provides the power needed to create an arc over the surface of a solid polytetrafluoroethylene (PTFE) propellant block. The arc ablates and ionizes small quantities of PTFE, resulting in a plasma. Since the plasma is conductive, the capacitor is then discharged through the plasma, which leads to the acceleration of the charged particles due to the magnetic field created by the discharge through the plasma. Figure 2 shows a schematic of a PPT and its circuitry.
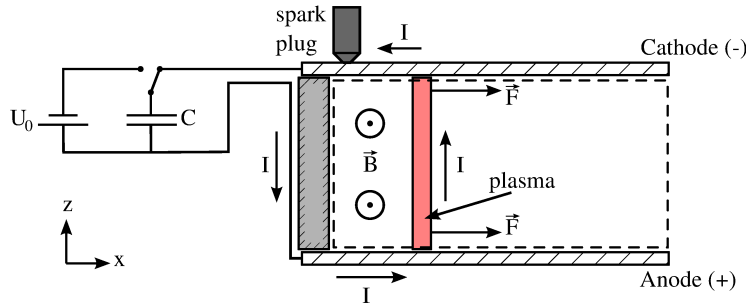

Figure 2. Schematic of the computational domain and the model of the PPT circuitry

Due to the inductance of the circuit, the current and the electrode voltage are described by a dampened oscillation, shown in Figure 3, which can be obtained by a fit to either experimental data or (in the case of Figure 3) to a simplified theoretical model, the so-called slug model.[12] At best, the current and voltage and the resulting electric and magnetic fields are computed directly based on the current state of the simulation. For testing purposes and in order to simplify the different components, methods have been implemented that allow the use of experimental data for different aspects of the simulation. Methods for varying degrees of realism have been implemented and are presented in the next sections.
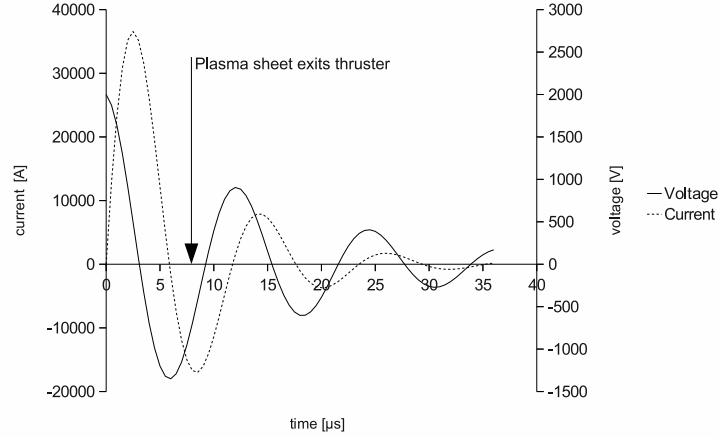
Figure 3. Fit function of a dampened oscillation of current and voltage for $I = a \cdot sin(b \cdot t) \cdot e^{c \cdot t}$ **and** $U = d \cdot cos(f \cdot t) \cdot e^{g \cdot t}$
with $a = 52000, b = 535000, c = -130000, d = 2000, f = 510000, g = -65000$

C.   Initial Conditions

Since the ablation of the PTFE due to the initial arc triggered by the spark plug is a very complex process, a detailed modeling was postponed to future activities and a simplified approach is used here. An experimentally determined mass bit is assumed to be fully dissociated and partly ionized and inserted in a cuboid initial plasma sheet (see Figure 4).
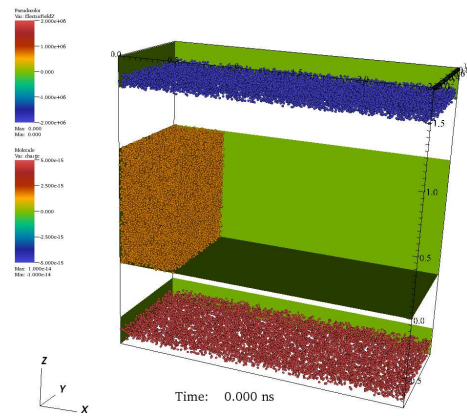

Figure 4. Exploded view of the initial condition in the thruster with electrodes: Electrons and ions pair-wise, on top of each other to achieve a neutral initial condition.

In a random setup of the charges in space, the electromagnetic field fluctuates wildly at the start of the simulation due to the immediate appearance of all particles in the first time step. In order to prevent this, the particles are kept from moving until the initial electromagnetic fields are developed fully within the computational domain. To further reduce initial disturbances, one ion and one electron each are placed at exactly the same position so there is no initial electric field from the particles, thus ensuring a homogeneous charge distribution.

D. Applied Voltage / Electrode Potential

The electrodes are connected to the power source for the discharge, a capacitor, and thus form an equipotential surface. The voltage $U(t)$, i.e. the potential difference, that has to be applied to the electrodes in the simulation, can be computed from the current I and the capacitance C of the capacitor according to

$$U(t) = U_0 - \frac{\int_0^t I\,dt}{C}. \tag{4}$$

Between the electrodes, an electric field is formed. This electric field is not homogeneous due to the charged particles moving in the space between the electrodes and because the electrodes themselves are not necessarily parallel, depending on the thruster type. Therefore, the potential difference has to be a boundary condition for the field solver and cannot simply be represented by a superimposed electric field. To apply a potential difference as boundary condition is natural for a numerical method solving the potential directly, such as a Poisson solver for the elliptic equation. However, applying this type of boundary condition to a hyperbolic solver (such as the one used in the context of this paper) is not trivial. While requiring a given boundary of arbitrary shape to be equipotential is as easy as formulating the corresponding characteristic boundary condition, forcing two equipotential surfaces on a given potential difference is problematic. The integral formulation of the potential surfaces would require an integration at least over each electrode as well as a line integral between the electrodes. Even this yields only the actual potential distribution. Reaching a certain prescribed potential difference is an additional challenge since a change in the boundary values or fluxes takes several iterations (depending on the discretization) to be propagated through the computational domain. Moreover, the transient and therefore strictly physical formulation of the hyperbolic Maxwell solver would be in conflict with an effectively elliptic boundary condition solver which would propagate information instantly over the whole domain.

Therefore, in the following, we investigate a different type of boundary condition for an applied potential which can be implemented in a hyperbolic solver. Physically, inside an electrode, charges are pushed onto it and distribute across the surface in such a way that each charge finds its equilibrium position, a position of minimal potential energy. Along the surface of the conducting material, the electromagnetic forces from all surrounding charges inside and outside the electrode cancel out each other, resulting in a surface of constant electric potential. As mentioned above, this result can be achieved in a hyperbolic Maxwell solver by imposing appropriate characteristic boundary conditions, enforcing the electric field to be oriented orthogonally to the surface. In a Particle-in-Cell code however, there is another way to model such a boundary condition. In a more natural way, the movable charges inside the electrode's conducting material are modeled directly in a simplified fashion. The self-consistent modeling allows each particle to move towards its equilibrium position, being pushed by the electromagnetic forces of the surrounding charges. If the potential difference between the electrodes is computed at each time interval i of a transient simulation, a desired voltage can be applied by controlling the total charge inside the electrodes. This charge can be varied by either changing the charge of each particle or by increasing or decreasing the number of particles inside the electrodes.

A simple way of computing the potential difference U between two points is to integrate the electric field along the straight line. In the context of this paper, the trapezoidal rule was used for the quadrature. Note that using this approach, the space along the line must lie completely within the computational domain.

For the control of the potential we propose a closed loop transfer function which is described in the following. A number of particles is deposited randomly within the electrodes. Particles in the cathode have a negative initial charge $-Q_0$, while particles inside the anode initially carry a positive charge Q_0. The potential difference U between the two electrodes is controlled by the charges of these particles. The charge Q_i is corrected each time interval i according to

$$Q_i = Q_{i-1} \cdot (1 + D_i). \tag{5}$$

with the change in charge at time interval i

$$D_i = \delta \cdot (U_{pr} - U_{av,i}) \cdot X_{av,i} , \tag{6}$$

where δ is a damping factor which is chosen to $\delta = 0.95$ in the context of this paper. Obviously, one important factor is the difference of the prescribed potential difference U_{pr} and the measured averaged potential difference $U_{av,i} = (1 - \frac{1}{n}) \cdot U_{av,i-1} + \frac{1}{n} \cdot U_i$, where n denotes the number of iterations over which

U is averaged. The other factor which enters in (6) is the averaged "inverse" potential difference $X_{av,i} = (1 - \frac{1}{n}) \cdot X_{av,i-1} + \frac{1}{n} \cdot X_i$, where

$$X_i = \frac{D_{i-1}}{(1 + D_{i-1})(U_{av,i} - U_{av,i-1})} \tag{7}$$

contains information about how to change the charge for a desired alteration in potential difference. This information is provided from previous time intervals where the charge in the electrodes has been adjusted. Clearly, X_i is not defined for $D_{i-1} = -1$ or $U_{av,i} = U_{av,i-1}$. Moreover, for the first iteration, D_{i-1} and $U_{av,i-1}$ are not defined. For these cases, the alternative computation of X_i is

$$X_i = \frac{1}{U_{pr}}. \tag{8}$$

This is to stabilize the controller so that the system does not become instable in the case of highly oscillating plasma flows inside the PPT.

In a simulation, an initial charge Q_i for the electrodes must be given. In a startup phase (mentioned already in section II.C), the control algorithm changes this charge so that the desired voltage is obtained. During this phase, the particles are not moved yet. Only at the end of the startup phase, all particles are released to move and be influenced by the surrounding electromagnetic fields.

It should be noted that the particles inside the electrodes are not allowed to move outside the electrode zones, which, for the particles, are bounded by reflective boundaries. The electromagnetic fields, however, are allowed to cross this boundary unperturbed.

E. Current and Magnetic Field

For a physically accurate simulation, the current has to be computed using the number of electrons leaving the cathode (and entering the anode). Since this requires a complex emission model for the cathode, a simpler model has been chosen preliminarily. In this model, it is assumed that any electron leaving the domain triggers the emission of a new electron from the cathode, keeping the overall charge in the plasma steady. The resulting current is computed by

$$I = \dot{n}_e \cdot q_e, \tag{9}$$

where $\dot{n}_e$ is the leaving number of electrons per time step and q_e is the charge of a single electron. Since it is entirely possible that the number of newly emitted electrons is not equal to the number of leaving electrons due to local potential variations, this is a very simplified approach that has to be replaced by an electron emission model eventually.

Alternatively, the current can be prescribed on the simulation. It is directly taken from a fit of a dampened oscillation to experimental or theoretical data in the form

$$I = a \cdot sin(b \cdot t) \cdot e^{c \cdot t}, \tag{10}$$

where a, b and c are constants derived from the fit. See Figure 3 for an example where the curve was fitted to the data from a simulation using the slug model.[12]

With either method, the current is deposited as current density in the cathode up to the position of the electron emission (see section II.F) and in the abstracted wire at the back of the PTFE propellant block. If a precomputed position of the plasma sheet is assumed, the current is deposited in the anode up to the assumed position. Otherwise, the positions of the electrons entering the anode are averaged over several time steps, yielding the position up to which the current in the anode is deposited. The placed current densities act as sources for the field solver in the same way as the particles, so that the magnetic field induced by the current has not to be computed separately. Alternatively, for testing purposes, the magnetic field can be computed from the current by computing the induced magnetic field with the well-known Biot-Savart equation.

F. Electron Emission

The number of emitted electrons in each time step is obtained directly from the current according to Eq. (9). The electrons are currently emitted with a Maxwellian velocity distribution based on the melting temperature of the cathode material (copper).

Since a detailed electron emission model is not implemented yet, three simplified models for the determination of the emission position of the electrons from the cathode have been tried.

The first is to predetermine the position in x-direction as function of time for a given thruster geometry and circuitry from the solution of the slug model.[12] The slug model assumes that the ablated plasma moves uniformly in the form of a plasma sheet towards the thruster exit. Solving the corresponding equations allows to determine the position of the plasma sheet and thus the emission position of the electrons at any given time. Using the predetermined time-dependent position in x-direction, the electrons are emitted randomly in a box of dimensions $d \times \Delta y \times d$ at the cathode boundary. $d << \Delta y$ is chosen according to geometry and discretization while Δy is the extent of the electrode in y-direction at the emission position $x(t)$. The second approach checks each element inside the cathode and identifies the element of highest absolute charge density. The electrons are emitted from the side of that element that is the boundary between computational domain and cathode zone.The third approach extends the second approach by extracting the charge that is emitted from the element of largest charge density and inserting that charge again at the entrance of the cathode ($x = 0$). This is done by deleting particles inside the emitting cathode element until the desired charge has been reached. The same number of particles is then introduced again into the cathode zone from the side, simulating them flowing onto the cathode from the capacitor.

III.   Results and Discussion

A.   Plasma Flow Simulation

The greatest challenge regarding the plasma modeling in simulating a PPT (or any large scale plasma application) using a particle approach is the prevention of instability due to very high electromagnetic fields. These basically originate from two closely related effects: Small cell sizes, which are necessary to accurately resolve the discontinuities in the plasma, lead to small distances between sampling points in the computational domains and therefore increased electromagnetic fields and a resulting instability of the simulation. At the same time, the particles cannot be simulated individually due to their large number but need to be combined into simulation particles using a so-called macro particle factor (MPF) which expresses the number of real particles represented by one simulated particles. An increasing MPF aggravates the first effect due to the concentration of the charge of a large number of real particles into a single simulated particle. These effects are especially pronounced when simulating a quasi neutral plasma since small local differences in the distribution of charged particles quickly lead to an instable spiral of ever higher electromagnetic fields and particle velocities. One approach to mitigate these effects is to represent the particles not as discrete points in space but as a charged volume. Several methods have been devised and implemented.[4] Figure 5 shows the deposited charges of a random distribution of ions and electrons in one dimension based on the deposition method. A total charge Q is represented by 100 positively charged particles and a total charge $-Q$ is represented by 100 negatively charged particles. All particles are positioned randomly in a one dimensional domain discretized by 5 grid cells. Due to the local distribution variations, the net charge in some grid cells is not equal to zero, leading to the aforementioned instability effects. The different deposition methods distribute the charges of the particles over a certain number of neighboring grid cells, effectively smoothing the charge distribution. Evidently this has the disadvantage of reduced spatial resolution and higher computational demand.

A second approach is to simply decrease the MPF. This evidently requires a higher number of simulated particles (for a given charge distribution). For most applications this approach is not feasible since the currently available computational power is far from sufficient.
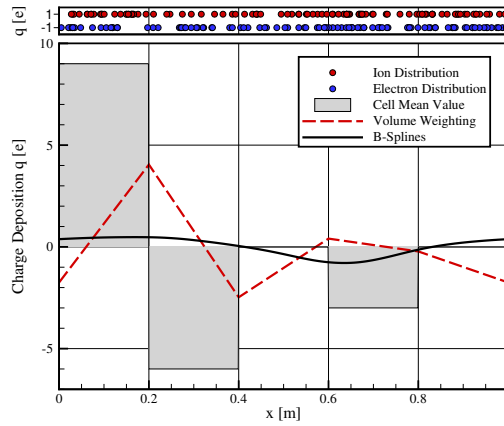
Figure 5. Effect of zero (cell mean value), first (volume weighting) and third (B-Splines) order charge deposition on the charge distribution of a quasi neutral plasma

B.   Initial Conditions

The ablation process at the start of a simulation is very simplified. Especially the degree of dissociation and ionization is unknown for specific thrusters. Also, a significant portion of the mass in reality is not contributing to the thrust efficiently due to particulate emissions and late term ablations,[13, 14] which are not considered in the currently used approach. Therefore, a complete ablation model would be necessary to implement all relevant effects. Since this is not feasible in the near term, a first step should be to identify the most prominent effects and find a way to model them at least approximately.

C.   Applied Voltage / Electrode Potential

Figure 6 shows the development of the potential between the electrodes and the correction factor in the first nanoseconds of a PPT simulation. At the very beginning ($t < 0.5\,\text{ns}$), the particles are kept from moving to allow the full development of the starting potential. As soon as the particles are set free, their movement leads to strong variations in the electromagnetic fields and, consequentially, the potential. As can be seen, the control algorithm described in Section II.D is able to quickly restore the desired electrode potential and keeps the potential accurate within certain limits. The limits depend on the settings for the transfer function (especially the number of changes to be averaged n and the damping factor δ) and the physical and numerical properties of the simulated plasma configuration. In the simulations that have been performed so far, typical deviations of the potential difference were between 15% and 25%. However, for some configurations, especially for low n and high δ, the control algorithm described in Section II.D has been observed to become unstable. The improvement of these settings is subject to future investigations.
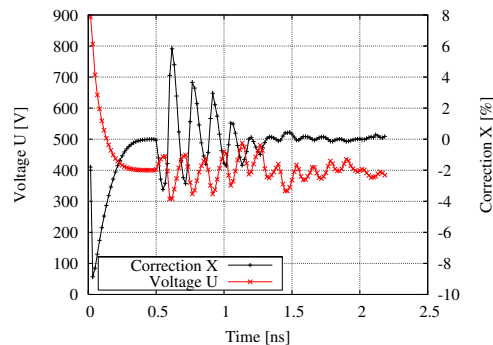

Figure 6.   During startup ($t < 0.5\,\text{ns}$), the potential is adjusted to the impressed value. After $t = 0.5\,\text{ns}$, the charged particles in the space between the electrodes are allowed to move and the potential between the electrodes is actively controlled to remain close to the here impressed potential of $400\,\text{V}$

D. Current and Magnetic Field

Figure 7 shows the result of a verification simulation for the magnetic field computation based on the current flowing through the capacitor according to Figure 2. Since the magnetic field of moving particles would interfere with the field from the current, no particles were inserted for this simulation. The hypothetical emission point of the electrons and therefore the position of the plasma sheet and the length of the current flow within the electrodes is derived from the previously mentioned slug model at an arbitrary time. The magnetic field and its propagation through the computational domain are not prescribed but computed by the field solver. The resulting magnetic field is in good agreement with the analytical solution of the Bio-Savart equation.
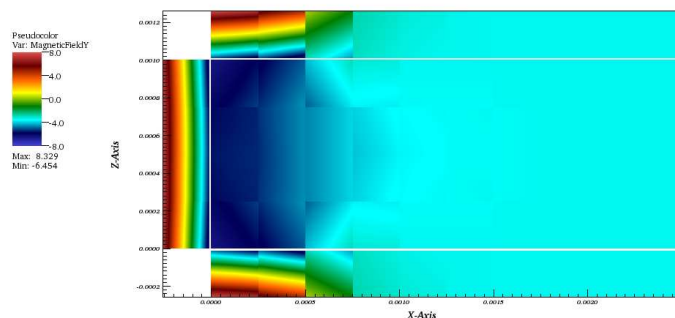

Figure 7. Magnetic field B_y due to deposited current densities deposited according to Figure 2. Two-dimensional view (slice in x-z-plane). White lines indicate the border of the plasma flow region.

E. Electron Emission

The most simple approach using a predetermined x-position for the emission has been found to be the most stable method. It works fine for the emission itself but risks inconsistencies in the simulation. The simulation follows the prescribed emission position but electrons are emitted ahead of the ions, dragging them through the thruster as seen in the snapshot in Figure 8.
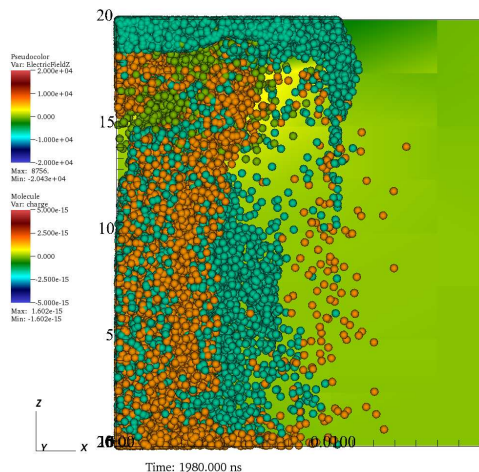

Figure 8. Electron emission at predetermined x-position: The electrons are inserted ahead of the plasma, dragging the ions toward the right as can be seen in the upper part of the domain.

The second approach showed the problem that particles were emitted all over the cathode instead of focusing on the region containing the ions as shown in Figure 9. This disadvantage was expected to be mitigated in the third approach. This approach works well for the start of the simulation, when the ions are

still at the backside as in Figure 9. However, the electrons are still emitted at the backside of the thruster even if the ions are already proceeded further in the thruster.
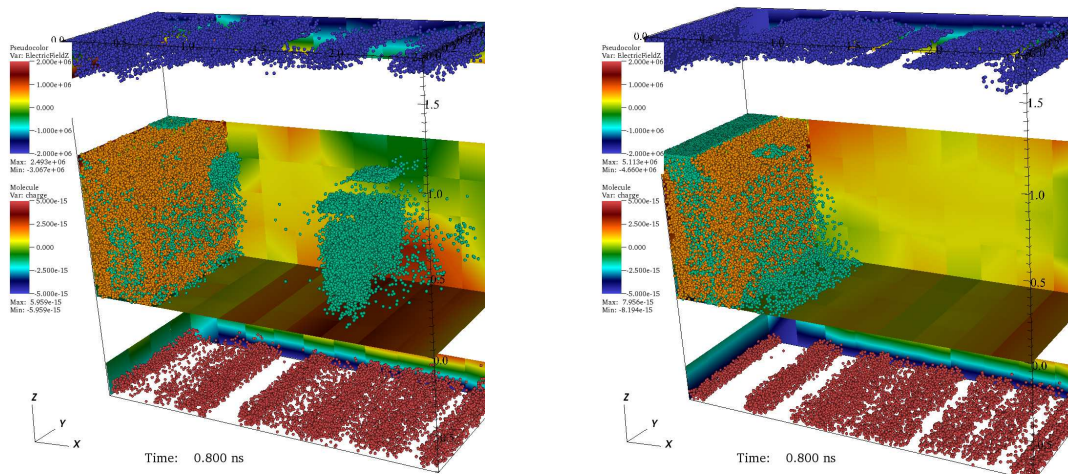

Figure 9. Exploded view of the thruster with electrodes: Emission without removing particles from the cathode (left) results in particles being emitted from boundary sides all over the cathode (instead of mainly at the position of the ions). In the case of emission with removal of charges from the cathode (right), this problem can be solved.

IV.   Conclusions and Outlook

The presented experiences with simlified PPT simulations offer a set of suggested methods for the three-dimensional modeling and simulation of a PPT. These methods include especially the circuitry beyond the actual computational domain such as a boundary condition for the transient, self-consistent applied potential difference in a hyperbolic solver. Different approaches for the electron emission have been tested. Though a complete, self-consistent simulation of a PPT has not been performed yet, an overview of the essential builing blocks was gained. One future goal is the simulation with a higher resolution both of the computational grid as also in terms of simulated particle number. Further investigations will also include the improvement of the control algorithm of the applied potential boundary condition as well as the improvement of the electron emission. Along with these, preliminary self-consistent PPT simulations without collisions can be performed.

Acknowledgments

References

[1]Nawaz, A., Albertoni, R., and Auweter-Kurtz, M., "Thrust efficiency optimization of the pulsed plasma thruster SIMP-LEX," *Acta Astronautica*, Vol. 67, No. 3-4, August-September 2010, pp. 440–448.

[2]Laufer, R., Bock, D., Lachenmann, M., and the Lunar Mission BW1 Project Team, "Academic Small Lunar Satellite Mission Concept and Design," IAC-08-B4.8.5, presented at the 59th International Astronautical Congress, Glasgow, UK, 2008.

[3]Neudorfer, J., Munz, C.-D., Stindl, T., Fertig, M., Roller, S., Schneider, R., and Auweter-Kurtz, M., "Particle In Cell Simulation Using a Discontinuous Galerkin Method," IEPC-2009-237, Proceedings of the 31th International Electric Propulsion Conference, Ann Arbor, MI, USA, 2009.

[4]Stindl, T., Neudorfer, J., Stock, A., Auweter-Kurtz, M., Munz, C., Roller, S., and Schneider, R., "Comparison of coupling techniques in a high-order discontinuous Galerkin based particle in cell solver," *J. Phys. D: Applied Physics*, Vol. 44, 2011, pp. 194004.

[5]Hockney, R. and Eastwood, J., *Computer Simulation using Particles*, McGraw-Hill, New York, 1981.

[6]Gassner, G., Lörcher, F., and Munz, C., "A Discontinuous Galerkin Scheme based on a Space-Time Expansion II. Viscous

Flow Equations in Multi Dimensions," *J. Sci. Comput.*, Vol. 34, No. 3, 2008, pp. 260–286.

[7]Munz, C.-D., Omnes, P., and Schneider, R., "A three-dimensional finite-volume solver for the Maxwell equations with divergence cleaning on unstructered meshes," *Computer Physics Communications*, Vol. 130, 2000, pp. 83 – 117.

[8]Fertig, M., Petkow, D., Stindl, T., Quandt, M., Munz, C.-D., Neudorfer, J., Roller, S., D'Andrea, D., and Schneider, R., "Hybrid Code Development for the Numerical Simulation of Instationary Magnetoplasmadynamic Thrusters," High Performance Computing in Science and Engineering '08, Springer, Berlin, Heidelberg, pp. 585–597, 2009.

[9]Petkow, D., *Partikelbasierte Modellierung und Simulation von hochverdünnten Plasmaströmungen*, Ph.D. thesis, In Preparation, Fakultät Luft- und Raumfahrttechnik und Geodäsie, Universität Stuttgart, Germany, 2010.

[10]D'Andrea, D., Munz, C.-D., and Schneider, R., "Modeling of Long-Range Intra- and Inter-Species Charged Particle Collisions for PIC Simulations," *Commun. Comput. Phys.*, Vol. 7, 2010, pp. 877–903.

[11]Stock, A., Neudorfer, J., Steinbusch, B., Stindl, T., Schneider, R., Roller, S., Munz, C.-D., and Auweter-Kurtz, M., "Three-Dimensional Gyrotron Simulation Using a High-Order Particle-In-Cell Method," *accepted for publication in High Performance Computing in Science and Engineering '11*, edited by W. E. Nagel, D. B. Kröner, and M. M. Resch, Springer Berlin Heidelberg.

[12]Jahn, R., *Physics of Electric Propulsion*, McGraw-Hill, New York, 1968.

[13]Spanjers, G. G., Lotspeich, J. S., McFall, K. A., and Spores, R. A., "Propellant Losses Because of Particulate Emission in a Pulsed Plasma Thruster," *Journal of Propulsion and Power*, Vol. 14, No. 4, July 1998, pp. 554–559.

[14]Spanjers, G. G., McFall, K. A., Gulczinski, F. S., I., and Spores, R. A., "Investigation of Propellant Inefficiencies in a Pulsed Plasma Thruster," AIAA-1996-2723, Proceedings of the 32nd AIAA/ASME/SAE/ASEE Joint Propulsion Conference and Exhibit, Lake Buena Vista, USA, 1996.